

1
2
3
4
5
6
7
8
9
10
11
12
13
14
15
16
17
18
19
20
21
22
23
24
25

Characteristics and source apportionment of fine haze aerosol in Beijing during the winter of 2013

Xiaona Shang¹, Kai Zhang^{2*}, Fan Meng², Shihao Wang², Meehye Lee^{1*}, Inseon Suh¹, Daegon Kim³, Kwonho Jeon³, Hyunju Park³, Xuezhong Wang², Yuxi Zhao²

¹ Department of Earth & Environmental Sciences, Korea University, Seoul, South Korea

² State Key Laboratory of Environmental Criteria and Risk Assessment, Chinese Research Academy of Environmental Sciences, Beijing 100012, China

³ Department of Climate & Air Quality Research, National Institution of Environmental Research, Incheon, South Korea

*Correspondence to: K. Zhang (zhangkai@craes.org.cn) or Meehye Lee (meehye@korea.ac.kr)

To be submitted to Atmospheric Chemistry and Physics

May 2017

26 **Abstract**

27

28 For PM_{2.5} filter samples collected daily at the Chinese Research Academy of Environmental
29 Sciences (Beijing, China) from December of 2013 to February of 2014 (the winter period),
30 chemical characteristics and sources were investigated with an emphasis on haze events in
31 different alert levels. During the three months, the average PM_{2.5} concentration was 89 μg m⁻³,
32 exceeding the Chinese national standard of 75 μg m⁻³ in 24 h. The maximum PM_{2.5}
33 concentration was 307 μg m⁻³, which characterizes *developed-type* pollution (PM_{2.5}/PM₁₀ >
34 0.5) in the World Health Organization criteria. PM_{2.5} was dominated by SO₄²⁻, NO₃⁻, and
35 pseudo-carbonaceous compounds with obvious differences in concentrations and proportions
36 between non-haze and haze episodes. The non-negative matrix factorization (NMF) analysis
37 provided reasonable PM_{2.5} source profiles, by which five sources were identified: soil dust,
38 traffic emission, biomass combustion, industrial emission, and coal combustion accounting
39 for 13 %, 22 %, 12 %, 28 %, and 25 %, respectively. The dust impact increased with
40 northwesterlies during non-haze periods and decreased under stagnant condition during haze
41 periods. A blue alert of heavy air pollution was characterized by the greatest contribution
42 from industrial emissions (61 %). During the Chinese Lantern Festival, an orange-alert was
43 issued and biomass combustion was found to be the major source owing to firecracker
44 explosions. Red-alert haze was almost equally contributed by local traffic and transported
45 coal combustion emissions from Beijing vicinities (approximately 40 % each) that was
46 distinguished by the highest levels of NO₃⁻ and SO₄²⁻, respectively. This study also reveals
47 that the severity and source of haze are largely dependent on meteorological conditions.

48

49 Key words: PM_{2.5}, winter haze, Beijing, chemical composition, source apportionment, NMF

50 **1. Introduction**

51

52 With the increasing PM_{2.5} concentration in northern China, winter haze occurrences increased
53 from 3 to 16 days per year during 2000–2012 (Wang and Chen, 2016). The frequency of haze
54 events during winter is enhanced by meteorological conditions; the minimum daily
55 temperatures typically reach –15 to –20 °C (Wu et al., 2012) and the boundary layer height
56 becomes shallow to less than 100 m (Zheng et al., 2015). Moreover, the combustion of fossil
57 fuel increases at low temperatures (Zhang and Samet, 2015). As the air quality deteriorated,
58 China released its third revision of the “The National Ambient Air Quality Standards”
59 (NAAQS) in 2012 (GB 3095-2012), which stipulated safe PM_{2.5} levels for the first time
60 (Zhang and Cao, 2015). However, the worst haze events in the major cities of China were
61 recorded during the winter of 2012–2013. During January of this period, Beijing experienced
62 almost daily haze and the hourly PM_{2.5} concentration reached 855 µg m⁻³ (Zheng et al., 2015).
63 In Beijing, winter haze episodes were 5 days in duration (Zheng et al., 2015, 2016). The long
64 duration of haze with high PM_{2.5} concentration triggers a red alert for air pollution (Liu et al.,
65 2017), which is the highest level of the heavy air pollution warning system issued in the
66 “Emergency plan for heavy air pollution in Beijing (revised in 2016)” (in Chinese:
67 <http://zhengce.beijing.gov.cn/library/192/33/50/200/806828/96701/index.html>).

68

69 The concentrations of SO₂, NO_x, and volatile organic compounds (VOCs), which are
70 important precursors of PM_{2.5}, vary in different emission and policy implementations. Related
71 particulate compositions (sulfate, nitrate, and organic matter) comprise two thirds of PM_{2.5}
72 (Huang et al., 2014; Hu et al., 2015). Over a seven-year period (2000–2006), SO₂ emission
73 has increased by 53 %, consistent with the increases in power plant emissions from 10.6 Tg to
74 18.6 Tg (Lu et al., 2010). Particularly in northern China, the emissions from power plants
75 have increased by 85 % over this period. In contrast, SO₂ levels have significantly decreased
76 since 2006, when stricter SO₂ regulations, such as the use of flue-gas desulfurization systems
77 or scrubbers, were imposed (Van der A et al., 2016). The reduction was particularly rapid
78 during 2008–2009. On the other hand, the NO_x concentration increased from 2000 to 2012
79 (Hong et al., 2016; Cao et al., 2011). This increase is in accord with the increased number of
80 vehicles, which contribute 90 % of the total NO_x emissions in Beijing (Hendrick et al., 2014;

81 Wu et al., 2012). Meanwhile, the continuous increase in VOC emissions (from 13 Tg/yr in
82 2000 to 26 Tg/yr in 2012) was mainly driven by industrial processes (~70 %) (Hong et al.,
83 2016). Coal combustion (especially that of raw coal) from households is underestimated in the
84 southern and eastern rural areas of Beijing. Rural coal combustion comprises approximately
85 75 % of Beijing's total coal combustion (Cheng et al., 2017). After the 2008 Olympic Games,
86 residential coal combustion emitted large amounts of SO₂, NO_x, and VOCs (70, 17, and 43 kt,
87 respectively). In 2013, these amounts had increased twofold to 132, 33, and 81 kt,
88 respectively. At the end of 2013, China issued the Air Pollution Prevention and Control
89 Action Plan (CAAC, 2013), which greatly reduced the precursor emissions in 2014 (Wang et
90 al., 2015).

91

92 Under the strict regulations on boiler and industrial emissions, SO₂ concentrations in Beijing
93 significantly decreased during the winter of 2013 and the fuel sulfur was reduced by more
94 than 80 % in 2014 (relative to its 2013 levels) (CAAC, 2013; CAAC, 2015). Over the same
95 period, the NO_x levels were reduced by 6.7 % over the nation, but exceeded the standard by
96 42 % in Beijing, where local traffic emissions remained high. Meanwhile, the PM_{2.5} pollution
97 is the most severe in the region of southern Beijing, where the annual average concentration
98 reached 150 µg m⁻³ during 2014–2015. The level is comparable to the national standard of
99 PM₁₀ (CAAC, 2015; Zhang and Cao, 2015).

100

101 Since the 2008 Olympics and 2013 CAACs, heavy industries have been relocated and high-
102 quality fuel has been introduced. Both actions have reduced the concentrations of gaseous
103 precursors (Wang et al., 2009; Van der A et al., 2016), although these reductions are in
104 contrast to the frequent hazes currently observed in Beijing. In recent studies, the PM_{2.5}, dust,
105 and SO₂ concentrations in Beijing have been mainly attributed to regional transport (Wang et
106 al., 2014; Yang et al., 2013; Wang et al., 2011). Considering the extreme haze situation in
107 Beijing, researchers have sought the crucial factors of haze formation, usually by identifying
108 the emission sources of PM_{2.5}. The source apportionment of PM_{2.5} is commonly analyzed by
109 source receptor models such as positive matrix factorization (PMF) and non-negative matrix
110 factorization (NMF) (Reff et al., 2007; Kfoury et al., 2016). These models have implicated
111 coal and industries as major sources of PM_{2.5} in Beijing (Huang et al., 2014; Zhang and Cao,

112 2015; Zhang et al., 2013).

113

114 Following the severe and frequent haze occurrences in January of 2013, the chemical
115 characteristics and sources of PM_{2.5} in Beijing were extensively investigated (Jiang et al.,
116 2015; Zheng et al., 2015; Zhang et al., 2015; Chen et al., 2017). However, few studies have
117 investigated the winter season of 2013–2014, which immediately followed the enactment of
118 the 2013 CAAC in China. In particular, the source apportionment of Beijing’s haze remains
119 unknown (Wu et al., 2016). In the present study, we thoroughly examine the chemical
120 compositions of PM_{2.5} in Beijing during the winter of 2013–2014, and accordingly, diagnose
121 the haze occurrence, probe the local and transported influence on haze, and quantify the
122 critical source contributions.

123

124 **2. Experiments**

125

126 Filtered samples of PM₁₀ and PM_{2.5} were collected on the roof of a three-story container (~15
127 m above ground level) at the Chinese Research Academy of Environmental Sciences (CRAES)
128 in Beijing, China (40.04 °N, 116.42 °E), from December of 2013 to February of 2014. The
129 site is located near the four-way intersection of a residential area located between the 5th and
130 6th ring roads of Beijing.

131

132 Aerosols were collected for 24 hours (from 7 pm to 7 pm next day) on a 90-mm
133 polypropylene filter using a medium volume sampler at a flow rate of ~100 L/min (2030,
134 Laoying, China). Seventy PM_{2.5} samples were collected and analyzed. The water-soluble ions
135 (Cl⁻, NO₂⁻, CO₃²⁻, SO₄²⁻, NO₃⁻, Na⁺, NH₄⁺, K⁺, Mg²⁺, and Ca²⁺) were measured by ion
136 chromatography (IC25, Dionex, USA) with a detection limit between 0.01 and 0.06 µg m⁻³.
137 The ionic measurement method is detailed in Lim (2009). For trace elemental analysis, the
138 samples were digested by a mixture of acids as described in Zhang et al. (2014). A quarter of
139 each filter was placed into a polytetrafluoroethylene flask and digested with 8 mL of
140 HNO₃/H₂O₂ (6/2 v/v, superpure grade, Merck, Darmstadt) at 180 °C for 8 h. The solution was
141 separated by centrifugation and diluted to 25 mL with ultrapure water. The concentrations of

142 trace metals (21 species, including Si) were determined by inductively coupled plasma-optical
143 emission spectrometry (Prodigy 7, Teledyne Leeman, USA). The mass concentration of PM₁₀
144 was also determined for comparison with that of PM_{2.5}.

145
146 The total concentrations of the water-soluble ions and trace elements were subtracted from the
147 PM_{2.5} mass, to provide a measure that likely represents the carbonaceous components that
148 were not directly measured. In this study, therefore, it was referred as the pseudo-
149 carbonaceous components and used for the following discussion. The concentrations of these
150 pseudo-carbonaceous components were comparable to those of PM_{2.5} concentrations observed
151 in Beijing (Ji et al., 2016). A meteorological suite of relative humidity, temperature, and
152 visibility was collected by CRAES from a sharing network of the China Meteorological Data
153 Service Center (CMDC): <http://data.cma.cn/en/?r=data/detail&dataCode=A.0012.0001>. The
154 gaseous species NO_x, SO₂, CO, and O₃ were measured using commercial analyzers (42i, 43i,
155 48i, 49i, Thermo Fisher, USA) in CRAES.

156
157 The PM_{2.5} source was identified by non-negative matrix factorization (NMF) analysis.
158 Introduced by Lee and Seung (1999, 2001), NMF operates similarly to positive matrix
159 factorization (PMF). Both analysis methods find two matrices (W and H, termed the
160 contribution matrix and the source profile matrix, respectively) that best reproduce the input
161 data matrix (V) using the same factorization approach ($V = WH$) as a positive constraint.
162 However, while PMF is a generalized, alternative least-squares method, NMF minimizes the
163 conventional least-squares error and the generalized Kullback–Leibler divergence. The
164 uncertainties in NMF analysis were estimated as 0.3 + the analytical detection limit (Xie et al.,
165 1999a, b).

166
167 In addition to NMF analysis, the origin of air masses was traced by trajectory analysis. For air
168 masses arriving at 500 m altitude, backward trajectories were computed for 72 hours using
169 HYSPLIT model with GDAS data in SplitR (Stein et al., 2015, [https://github.com/rich-](https://github.com/richiannone/SplitR)
170 [iannone/ SplitR](https://github.com/richiannone/SplitR)).

171

172 3. Characteristics of winter PM_{2.5}

173 3.1. PM_{2.5} and PM₁₀ mass variations

174

175 During the 2013–2014 winter period in Beijing, the mass concentrations of PM_{2.5} and PM₁₀
176 varied in a similar pattern (Fig. 1). Zheng et al. (2015) reported a similar trend between the
177 PM_{2.5} and PM₁₀ concentrations. In this study, the average PM₁₀ concentration was 142 $\mu\text{g m}^{-3}$,
178 comparable to the Chinese national standard of 150 $\mu\text{g m}^{-3}$ in 24 h (GB 3095-2012). However,
179 the mean PM_{2.5} concentration was 89 $\mu\text{g m}^{-3}$, exceeding the standard of 75 $\mu\text{g m}^{-3}$ in 24 h.
180 The PM_{2.5} standard was most severely exceeded in February 2014, when the average
181 concentration (133.5 $\mu\text{g m}^{-3}$) reached the highest winter concentration in Beijing during the
182 2005–2015 decade (Lang et al., 2017).

183

184 Based on the criteria of the World Health Organization (WHO) (2006), the wintertime air
185 pollution of Beijing was classified as *developed-type*, meaning that the PM_{2.5}/PM₁₀ ratio
186 exceeded 0.5 in 70 % of the samples (Table 1). The mean PM_{2.5} concentration of these
187 samples (113 $\mu\text{g m}^{-3}$) was four times higher than that in *developing-type* pollution (31 $\mu\text{g m}^{-3}$).
188 In approximately half of the *developed-type* samples, the PM_{2.5} and PM₁₀ mass concentrations
189 exceeded the national standards, all of which were collected during haze events. The average
190 PM_{2.5} concentration over 13 haze days reached 198 $\mu\text{g m}^{-3}$ and the visibility was significantly
191 reduced to ~ 1 km (Fig. 1). In contrast, the PM_{2.5} concentration exceeded the standard without
192 violating the PM₁₀ concentration on only a few days. These results well reflect the wintertime
193 characteristics of PM_{2.5} levels in Beijing, which are largely related to haze episodes. The
194 average PM_{2.5} concentration of the *developed-type* was comparable to that of the *developing-*
195 *type* unless the PM_{2.5} concentration exceeded the standard.

196

197 On 12 out of 13 haze days, the pollutant levels met the criteria of heavy air pollution alerts
198 stipulated in the “Emergency plan for heavy air pollution in Beijing (revised in 2016)”. In the
199 lowest level of the four-tier warning system, blue alert, the daily average air quality index
200 (AQI) exceeded 200 on only one day. In Table 1, the one no-alert and three blue-alert haze
201 days are defined as no/blue-alert haze events. The average PM_{2.5} concentration on these days
202 was 168 $\mu\text{g m}^{-3}$ (Table 1). During the red-alert period (February 20–25), the daily PM_{2.5}

203 concentration peaked at $306 \mu\text{g m}^{-3}$. A red alert is declared when the air pollution is heavy and
204 severe. During a red alert, AQI exceeds 200 on four consecutive days and exceeds 300 on
205 continuous two of those days. Although the daily average AQI remained higher than 300
206 during the February 14–16 period, this event was an orange alert because it continued for only
207 three days. The AQI data can be found at [http://www.tianqihoubao.com/aqi/beijing-](http://www.tianqihoubao.com/aqi/beijing-201402.html)
208 [201402.html](http://www.tianqihoubao.com/aqi/beijing-201402.html) (in Chinese). Here, we describe episodes in terms of alerts defined in the heavy
209 air pollution system rather than in the haze alert system, because the former definition is
210 based on the daily averaged AQI, whereas the three-tier haze warnings depend on the hourly
211 meteorological parameters (relative humidity and visibility) or $\text{PM}_{2.5}$. Because we measured
212 the daily concentrations, the heavy air pollution alert was suitable for our purpose.

213 **3.2. Chemical composition**

214
215 Throughout the wintertime, the average $\text{PM}_{2.5}$ concentration remained close to $90 \mu\text{g m}^{-3}$, 20 %
216 above the national standard. The major $\text{PM}_{2.5}$ components were SO_4^{2-} , NO_3^- , NH_4^+ , and
217 pseudo-carbonaceous compounds, with average concentrations of 18.8, 16.9, 8.5, and $38.6 \mu\text{g}$
218 m^{-3} , respectively. Collectively, these four compositions comprised 83 % of the $\text{PM}_{2.5}$ mass
219 (Fig. 2). On the 57 non-haze days, the fractional chemical compositions and concentrations of
220 SO_2 and NO_2 were comparable to those of the entire period (70 days). In contrast, the portions
221 of soil minerals such as Ca^{2+} and trace elements (including Si) were 3–4 times higher on non-
222 haze days than on haze days. The Ca^{2+} and Si concentrations were highly correlated ($r^2 = 0.8$)
223 and were more related to the PM_{10} ($r^2 = 0.6$) than $\text{PM}_{2.5}$ levels. This reflects the significant
224 impact of soil dust on non-haze days (Fu et al., 2012). On haze days, the particle masses,
225 compositions, SO_2 , and NO_2 varied widely among the different alert levels.

226

227 **3.3. Source profiles**

228

229 The $\text{PM}_{2.5}$ sources were identified in an NMF analysis of the measurement data. The data
230 included 8 water-soluble ions, 13 trace elements, and pseudo-carbonaceous compounds. After
231 comparison through a principle component analysis, the principal factors were determined.

232 Finally, five critical factors were distinguished: soil dust, traffic emission, biomass
233 combustion, industrial emission, and coal combustion (Table 2). The five source profiles are
234 presented in Figure 3. Despite their clear signatures, the contributions of dust and traffic
235 emissions were approximately half those of biomass combustion, industrial emission, and
236 coal combustion (Table 2).

237

238 Factor 1 (soil dust) is confirmed by high Ca^{2+} , Si, Fe, Cl^- , and Na^+ contents (Fu et al., 2012).
239 The high concentrations of Cl^- and Na^+ likely originate from dry lake deposits (Abuduwaili et
240 al., 2015), which spread over the northern area of Beijing. Elevated heavy metals suggest the
241 presence of fugitive dust mixed with industry or traffic emissions (Wan et al., 2016). The high
242 loadings of NO_3^- and NH_4^+ in Factor 2 indicate traffic emissions (He et al., 2016). As is well
243 known, NH_3 is emitted from three-way catalytic converters in vehicles (Chang et al., 2016).
244 Factor 3 (biomass combustion) emits large amounts of K^+ and NH_4^+ (Balasubramanian et al.,
245 1999), along with the elements that give exploding fireworks their color (namely Mg, Fe, Al,
246 Ti, Cu, and Si) (Baranyai et al., 2015). The concentrations of these firecracker indicators are
247 most significantly elevated during the Chinese Lantern Festival (14, 15, and 16 of February;
248 Fig. 1). Factor 4 (industrial emissions) is distinguished by high pseudo-carbonaceous
249 materials and heavy metals. Factor 5 (coal combustion) is characterized by high Cl^- , SO_4^{2-} ,
250 and NO_3^- contributions, which are absent in Factor 4. Although both Factors 4 and 5 represent
251 the influence of industrial emissions near Beijing, Factor 5 is more clearly sourced from
252 industries requiring high energy, such as iron and steel, cement, and power plants (Tan et al.,
253 2016; Zhang et al., 2013). In contrast, Factor 4 indicates emissions from industrial processes
254 using VOCs as raw materials such as furniture manufacturing, petroleum refining, machinery
255 equipment manufacturing and printing (Wu et al., 2015).

256

257 In a previous study, source apportionment by NMF or PMF analysis distinguished 7–8 factors
258 (Zhang et al., 2013), including a secondary formation source. The secondary source was not
259 separated as an individual factor in the present study. As a typical secondary species, SO_4^{2-}
260 dominates in Factor 5. However, a NO_3^- signature appears in all factors except Factor 4. As a
261 megacity, Beijing is surrounded by large satellite cities with industrial complexes. Thus,
262 Beijing is susceptible to emissions from these areas in addition to its own emissions, when

263 meteorological conditions are met. This will be discussed in detail in the following section. In
264 fact, the atmospheric condition facilitated haze occurrence, leading to the major sources and
265 the degree of aging for aerosols being intimately coupled. Therefore, these five factors
266 primarily represent direct emission sources with secondary sources being implicitly included.
267 In addition, NO₂ is more likely sourced from local emissions, but SO₂ is expected to be
268 transported from nearby regions.

269

270 **4. Characteristics of winter haze**

271 **4.1. Chemical and meteorological characteristics**

272

273 The chemical compositions of PM_{2.5} clearly differed on haze in contrast to non-haze days in
274 terms of secondary ions and pseudo-carbonaceous compounds (Fig. 2). The largest fraction of
275 pseudo-carbonaceous compounds (61 %) was accompanied with the smallest proportion of
276 SO₄²⁻ (4%) on no/blue-alert days, suggesting low coal consumption by high-VOC-emitting
277 industries. On orange-alert haze events, the NO₃⁻ fraction was twice that on non-haze days,
278 and the K⁺ and Mg²⁺ proportions were maximized (at 6 % and 1 %, respectively), implying
279 biomass-combustion emission during the Lantern festival in China. The concentrations of
280 SO₄²⁻ and NO₃⁻ were comparable with the greatest contribution in red-alert haze events. In
281 addition, these species were closely related to the Cl⁻ ($r^2 = 0.8$) and NH₄⁺ ($r^2 = 0.9$)
282 concentrations, respectively, suggesting large contributions by coal combustion and vehicle
283 emission. It is also noteworthy that the SO₄²⁻ fraction varied more widely than the NO₃⁻
284 fraction (Table S1). Among the three levels of haze events, SO₄²⁻ varied from 4 % to 32 %,
285 whereas NO₃⁻ varied from 16 % to 31 % and NH₄⁺ from 9 % to 11 %. Similarly, although
286 both SO₂ and NO₂ concentrations were the highest in red-alert haze, SO₂ enhancement
287 (relative to non-haze days) was 20 % larger than NO₂ enhancement. Because the sulfur
288 compounds were much more elevated than the nitrogen compounds on haze days (particularly
289 in red-alert haze events), the winter haze in Beijing was concluded to be largely contributed
290 by coal combustion, which emits sulfur compounds. Furthermore, coal emissions are mostly
291 transported from nearby Beijing (Hendrick et al., 2014).

292

293 To examine the meteorological conditions favorable for haze occurrence and clarify the

294 emission source regions, surface weather maps combined with daily average backward
295 trajectories at 500 m were compared during non-haze and haze events. Previous studies also
296 reported that weather conditions were critical for haze formation. In East China, migratory
297 anticyclones and weak pressure gradients were the prerequisites of winter haze from 1980 to
298 2012 (Peng et al., 2016). High PM_{2.5} episodes in Beijing usually began with weak southerly
299 winds and ended with strong northerly winds (Guo et al., 2014). In this study, the air mass
300 was usually transported from the northwest. As the high pressure system expanded, however,
301 it was transported from the west, southwest, and southeast. Throughout this process, the
302 weather condition became increasingly stagnant (Fig. 4) and the haze-alert level increased
303 gradually. The recent study also emphasized the effect of meteorological condition on the
304 severity of haze in Beijing (Cai et al., 2017). When air masses were rapidly transported from
305 the northern desert area (Fig. 4a), mineral species such as Ca²⁺ and Si were enriched on non-
306 haze days and the PM₁₀ mass was high. In the western regions of Beijing (Fig. 4b), where
307 various industries manufacture food, drink, furniture, pharmaceuticals, and other products
308 from VOCs (<http://www.berkeleysg.com/2016/06/china-manufacturing-distribution-map/>),
309 the fraction of pseudo-carbonaceous compounds rose to its maximum as the air mass slightly
310 lingered over the region. During February 14–16, firecracker explosions caused a spike in K⁺,
311 Mg²⁺, and NH₄⁺ concentration under the stagnant weather condition, in which the air mass
312 moved very slowly from the southwestern areas, where population density is the highest
313 (Cheng et al., 2017). As the air mass moved eastward toward the high energy-requiring
314 regions (<http://berc.berkeley.edu/energy-access-developing-parts-china/>) (Fig. 4d), such as
315 Tianjin and Tangshan, where coal consumption is high for industrial use and residential
316 heating (Cheng et al., 2017), the PM_{2.5} and SO₄²⁻ (SO₂) concentrations reached their maxima.

317

318 **4.2. Source profiles**

319

320 To quantify each source contribution during the winter haze in Beijing, daily samples were
321 analyzed by NMF and the source profiles during haze and non-haze episodes were compared
322 (Fig. 5). In all samples, the main contributions were industrial, traffic, and coal combustion
323 emissions (22–28 %), followed by soil dust and biomass combustion (13 % and 12 %, respectively).
324 However, soil dust loading, which is associated with elevated fractions of Ca,

325 Si, and pseudo-carbonaceous matters (Fig. 2), was enhanced to 20 % during non-haze events.
326 Meanwhile, the local traffic contribution decreased as the air mass was rapidly transported
327 from the northwestern desert areas, as mentioned in subsection 4.1.

328

329 The three types of haze episodes exhibited strong contrasts not only in their chemical species
330 and source regions, as mentioned above, but also in their source profiles (Fig. 5). No/blue-
331 alert haze was dominated by industrial emissions (61 %) as the airflow passed over the
332 industrial regions manufacturing products from raw VOCs. Consequently, the pseudo-
333 carbonaceous concentration increased. During orange- and red-alert haze events, the dust
334 contribution was negligible and the anthropogenic fraction increased sharply. During the
335 Chinese Lantern Festival (which triggered an orange alert), a biomass signature with the
336 highest K^+ concentration was observed in the air mass transported from the southwestern
337 populated areas of Beijing. The K^+ contribution (35 %) was three times higher than that on
338 non-haze days. During February 20–25, the outflow of the high coal-consuming eastern
339 region enhanced the proportion of coal combustion products to 37 %. Simultaneously, the
340 traffic contribution was the highest at 43 %. The coal and traffic effects were accompanied by
341 two-fold elevations of SO_4^{2-} and NO_3^- in $PM_{2.5}$.

342

343 **5. Policy implications**

344

345 During the 2013–2014 winter period in Beijing, the average $PM_{2.5}$ concentration exceeded the
346 standard by 20 %, and in February, reached its highest level in the 2005–2015 decade (Lang
347 et al., 2017). The $PM_{2.5}$ mass closure and concentration of gaseous precursors during the 57
348 non-haze days were comparable to those of the entire winter period. Mineral dust is an
349 important source of $PM_{2.5}$ and elevates the PM_{10} concentration on non-haze days. The average
350 $PM_{2.5}$ concentrations increased significantly from $65 \mu g m^{-3}$ on non-haze days to $168 \mu g m^{-3}$
351 on no/blue-alert days and to $218 \mu g m^{-3}$ on red-alert days.

352

353 When weather conditions stagnate under weak pressure gradients, the alert levels of heavy air
354 pollution upgrade on haze days. The migratory anticyclones also shift the air masses, causing

355 wide variations in chemical species and emission sources. During haze days, the NO₂ and
356 NO₃⁻ concentrations exceed those of SO₂ and SO₄²⁻, respectively, but the sulfur-containing
357 species vary more widely than the nitrogen species. The sulfur compounds are particularly
358 enhanced in stagnant air masses transported from the Beijing vicinities, including the southern
359 and eastern regions, leading to the large sulfur variation with little change in nitrogen. These
360 results highlights the significant influence of the emissions from industries requiring high
361 energy and using coal in Beijing vicinities and from local vehicles on winter haze formation
362 in Beijing, which is in accordance with findings from previous studies (Hendrick et al., 2014;
363 Wang et al., 2016). To abate the severe haze in Beijing, therefore, it is necessary to reduce
364 vehicle emissions in Beijing and further sulfur emissions from industrial complexes and
365 uncontrolled coal combustion in surrounding cities. For cost-effectiveness, the weather
366 forecast needs to be incorporated into the policy implementation.

367

368 **6. Conclusion**

369

370 This study investigated the chemical characteristics of PM_{2.5} during the 2013–2014 winter
371 period in Beijing and identified its sources with an emphasis on haze events by measuring the
372 particle masses, water-soluble ions, and trace elements in filtered samples. Finally, policy
373 implications for controlling haze occurrences in Beijing were deduced from the analysis.

374

375 The samples were collected daily at CRAES, Beijing, China, from December of 2013 to
376 February of 2014. During the winter period, the overall average PM_{2.5} concentration in
377 Beijing was 89 μg/m³, exceeding the Chinese national standard of 75 μg/m³ in 24 h. The
378 excess was linked to high occurrence of haze events in February of 2014. The high PM_{2.5}
379 episodes were concurrent with PM₁₀ exceedance. Seventy percent of the samples were
380 identified as *developed-type* in the WHO criteria; that is, their PM_{2.5}/PM₁₀ ratios exceeded 0.5.
381 All 13 recognized haze events in this study were included in the *developed-type*.

382

383 The chemical compositions showed that secondary ions were doubled on haze days relative to
384 non-haze days, but mineral species were halved during haze events. For the 70 daily PM_{2.5}

385 samples, NMF analysis was performed and the source profiles were compared between haze
386 and non-haze days. The analysis identified five principle sources, of which industrial emission,
387 coal combustion, and traffic emission comprised similar fractions of 28 %, 25 %, and 22 %,
388 respectively. The soil-dust and biomass-combustion sources were well distinguished and
389 contributed 13 % and 12 %, respectively. Comparing the source profiles between non-haze
390 and haze events, the impact of soil dust was most noticeable on non-haze days, when the air
391 masses rapidly transported from northwestern desert areas and brought high concentrations of
392 Ca^{2+} and Si into Beijing. However, nearby transport of industrial, biomass combustion, and
393 coal combustion emissions, along with local traffic emission, contributed to haze events under
394 stagnant weather conditions. The contributions of these four sources increased by up to 61 %,
395 35 %, 37 %, and 43 % in no/blue-alert, orange-alert, and red-alert days, respectively. The
396 industries that are mainly located to the west of Beijing use VOCs as raw materials, elevating
397 the pseudo-carbonaceous components in $\text{PM}_{2.5}$. Biomass combustion increases during the
398 firework displays of the Lantern Festival (February 14–16). At that time, the K^+ and Mg^{2+}
399 concentrations are maximized. When a red-alert was issued for six days in 2014, the
400 contribution of SO_4^{2-} and NO_3^- increased by factors of 3 and 2, respectively, from their non-
401 haze levels. Overall, the sulfur compounds (SO_2 and SO_4^{2-}) varied much more widely than the
402 nitrogen compounds (NO_2 and NO_3^-) through haze events, implying the substantial
403 contribution of industrial emissions from coal combustion in surrounding cities. The high
404 level of nitrogen compounds suggests local vehicle emissions as a main source of winter haze
405 in Beijing. This study also emphasizes the role of weather condition in haze formation by
406 building up stagnant condition that facilitates the transport of industrial emissions from
407 Beijing vicinities. These findings will be applicable to policy making.

408

409

410 **Acknowledgements**

411

412 This study was performed via the China-Korea Air Quality Joint Research. A special thank
413 should be given to the Chinese Research Academy of Environmental Sciences (CRAES)
414 members including Pengli Duan, Fenmei Xia, Hongjiao Li, Zilong Zheng, Jing Zhou,
415 Qingshu Ke, Jiaying Yang, and Jikang Wang, for helping sampling in Beijing. K. Zhang

416 would like to acknowledge supports from the National Natural Science Foundation of China
417 (No. 41205093), the National Department Public Benefit Research Foundation (No.
418 201109005), and the Fundamental Research Funds for Central Public Welfare Scientific
419 Research Institutes of China (No. 2016YSKY-025). This work was supported by a grant from
420 the National Institute of Environmental Research (NIER), funded by the Ministry of
421 Environment (MOE) of the Republic of Korea (NIER-2007-03-02-011). M. Lee also thanks
422 for the support by Basic Science Research Program through the National Research
423 Foundation of Korea (NRF) funded by the Ministry of Science, ICT & Future Planning
424 (2017012143).

425 **References**

- 426 Abuduwaili, J., Zhaoyong, Z., Jiang, F., and Liu, D.: The disastrous effects of salt dust
427 deposition on cotton leaf photosynthesis and the cell physiological properties in the Ebinur
428 basin in northwest China, *PloS one*, 10, e0124546, doi.org/10.1371/journal.pone.0124546,
429 2015.
- 430 Balasubramanian, R., Victor, T., and Begum, R.: Impact of biomass burning on rainwater
431 acidity and com-position in Singapore, *J. Geophys. Res.*, 104, 26881-26890, doi:
432 10.1029/1999JD900247, 1999.
- 433 Baranyai, E., Simon, E., Braun, M., Tóthmérész, B., Posta, J., and Fábíán, I.: The effect of a
434 fireworks event on the amount and elemental concentration of deposited dust collected in
435 the city of Debrecen, Hungary, *Air Qual. Atmos. Health*, 8, 359-365, doi:10.1007/s11869-
436 014-0290-7, 2015.
- 437 CAAC 2013, Clean Air Alliance of China, State Council air pollution prevention and control
438 action plan, issue II, October 2013, <http://en.cleairchina.org/product/6346.html> (English
439 translation). Last accessed: 8 October 2015.
- 440 CAAC 2015, Clean Air Alliance of China, China Air Quality Management Assessment
441 Report, Issue II, December 2015, <http://en.cleairchina.org/product/7386.html> (English
442 translation).
- 443 Cai, W., Li, K., Liao, H., Wang, H., and Wu, L.: Weather conditions conducive to Beijing
444 severe haze more frequent under climate change, *Nat. Clim. Change*, 7, 257–262,
445 doi:10.1038/nclimate3249, 2017.
- 446 Cao, G. L., Zhang, X. Y., Gong, S. L., An, X. Q., and Wang, Y. Q.: Emission inventories of
447 primary particles and pollutant gases for China, *Chinese Sci. Bull.*, 56, 781–788,
448 doi:10.1007/s11434-011-4373-7, 2011.
- 449 Chang, Y., Zou, Z., Deng, C., Huang, K., Collett, J. L., Lin, J., and Zhuang, G.: The
450 importance of vehicle emissions as a source of atmospheric ammonia in the megacity of
451 Shanghai, *Atmos. Chem. Phys.*, 16, 3577–3594, doi:10.5194/acp-16-3577-2016, 2016.
- 452 Chen, F., Zhang, X., Zhu, X., Zhang, H., Gao, J., and Hopke, P. K.: Chemical characteristics
453 of PM_{2.5} during a 2016 winter haze episode in Shijiazhuang, China, *Aerosol Air Qual. Res.*,
454 17, 368-380, doi: 10.4209/aaqr.2016.06.0274, 2017.

455 Cheng, M., Zhi, G., Tang, W., Liu, S., Dang, H., Guo, Z., and Meng, F.: Air pollutant
456 emission from the underestimated households' coal consumption source in China, *Sci.*
457 *Total Environ.*, 580, 641-650, 2017.

458 Fu, Z., Zhai, Y., Wang, L., Zeng, G., Li, C., Peng, W., and Lu, P.: Morphological,
459 geochemical composition and origins of near-surface atmospheric dust in Changsha city of
460 China, *Environ. Earth Sci.*, 66, 2207-2216, doi:10.1007/s12665-011-1442-9, 2012.

461 Guo, S., Hu, M., Zamora, M. L., Peng, J., Shang, D., Zheng, J., and Molina, M. J.:
462 Elucidating severe urban haze formation in China, *Proc. Natl. Acad. Sci.*, 111, 17373-
463 17378, doi: 10.1073/pnas.1419604111, 2014.

464 He, J., Wu, L., Mao, H., Liu, H., Jing, B., Yu, Y., Ren, P., Feng, C., and Liu, X.:
465 Development of a vehicle emission inventory with high temporal-spatial resolution based
466 on NRT traffic data and its impact on air pollution in Beijing – Part 2: Impact of vehicle
467 emission on urban air quality, *Atmos. Chem. Phys.*, 16, 3171-3184, doi:10.5194/acp-16-
468 3171-2016, 2016.

469 Hendrick, F., Müller, J.-F., Clémer, K., Wang, P., De Mazière, M., Fayt, C., Gielen, C.,
470 Hermans, C., Ma, J. Z., Pinardi, G., Stavrou, T., Vlemmix, T., and Van Roozendaal, M.:
471 Four years of ground-based MAX-DOAS observations of HONO and NO₂ in the Beijing
472 area, *Atmos. Chem. Phys.*, 14, 765-781, doi:10.5194/acp-14-765-2014, 2014.

473 Hong, C., Zhang, Q., He, K., Guan, D., Li, M., Liu, F., and Zheng, B.: Variations of China's
474 emission estimates response to uncertainties in energy statistics, *Atmos. Chem. Phys.*
475 *Discuss.*, doi:10.5194/acp-2016-459, in review, 2016.

476 Hu, G., Sun, J., Zhang, Y., Shen, X., and Yang, Y.: Chemical composition of PM_{2.5} based on
477 two-year measurements at an urban site in Beijing, *Aerosol Air Qual. Res.*, 15, 1748-1759,
478 doi: 10.4209/aaqr.2014.11.0284, 2015.

479 Huang, R. J., Zhang, Y., Bozzetti, C., Ho, K. F., Cao, J. J., Han, Y., and Zotter, P.: High
480 secondary aerosol contribution to particulate pollution during haze events in China, *Nature*,
481 514, 218-222, doi:10.1038/nature13774, 2014.

482 Ji, D., Zhang, J., He, J., Wang, X., Pang, B., Liu, Z., and Wang, Y.: Characteristics of
483 atmospheric organic and elemental carbon aerosols in urban Beijing, China, *Atmos.*
484 *Environ.*, 125, 293-306, doi.org/10.1016/j.atmosenv.2015.11.020, 2016.

485 Jiang, J., Zhou, W., Cheng, Z., Wang, S., He, K., and Hao, J.: Particulate matter distributions
486 in China during a winter period with frequent pollution episodes (January 2013), *Aerosol*
487 *Air Qual. Res.*, 15, 494-503, doi: 10.4209/aaqr.2014.04.0070, 2015.

488 Kfoury, A., Ledoux, F., Roche, C., Delmaire, G., Roussel, G., and Courcot, D.: PM_{2.5} source
489 apportionment in a French urban coastal site under steelworks emission influences using
490 constrained non-negative matrix factorization receptor model, *J. Environ. Sci.*, 40, 114-128,
491 doi.org/10.1016/j.jes.2015.10.025, 2016.

492 Lang, J., Zhang, Y., Cheng, S., Zhou, Y., Chen, D., Guo, X., Li, X., Xing, X., Chen, S., and
493 Wang, H.: Trends of PM_{2.5} and chemical composition in Beijing, 2000-2015, *Aerosol Air*
494 *Qual. Res.*, 17, 412–425, doi: 10.4209/aaqr.2017.01.0042, 2017.

495 Lee, D. D. and Seung, H. S.: Learning the parts of objects by non-negative matrix
496 factorization, *Nature*, 401, 788-791, doi:10.1038/44565, 1999.

497 Lee, D. D. and Seung, H. S.: Algorithms for non-negative matrix factorization, *Adv. Neural*
498 *Inf. Process Syst.*, 13, 556–562, 2001.

499 Liu, T., Gong, S., He, J., Yu, M., Wang, Q., Li, H., Liu, W., Zhang, J., Li, L., Wang, X., Li, S.,
500 Lu, Y., Du, H., Wang, Y., Zhou, C., Liu, H., and Zhao, Q.: Attributions of meteorological
501 and emission factors to the 2015 winter severe haze pollution episodes in China's Jing-Jin-
502 Ji area, *Atmos. Chem. Phys.*, 17, 2971-2980, doi:10.5194/acp-17-2971-2017, 2017.

503 Lim, S.: Source Signature of Ions and Carbonaceous Compounds in Submicron and
504 Supermicron Aerosols at Gosan-super site, Jeju, South Korea, Master's thesis, Korea
505 University, 2009.

506 Lu, Z., Streets, D. G., Zhang, Q., Wang, S., Carmichael, G. R., Cheng, Y. F., Wei, C., Chin,
507 M., Diehl, T., and Tan, Q.: Sulfur dioxide emissions in China and sulfur trends in East
508 Asia since 2000, *Atmos. Chem. Phys.*, 10, 6311-6331, doi:10.5194/acp-10-6311-2010,
509 2010.

510 Ministry of Environmental Protection of the People's Republic of China, Ambient air quality
511 standards (GB3095-2012), Chinese Environmental Science Press: Beijing, China, 2012 (in
512 Chinese).

513 Peng, H., Liu, D., Zhou, B., Su, Y., Wu, J., Shen, H., Wei, J., and Cao, L.: Boundary-layer
514 characteristics of persistent regional haze events and heavy haze days in eastern China,

515 Adv. Meteorol., 6950154, doi.org/10.1155/2016/6950154, 2016.

516 Reff, A., Eberly, S., and Bhawe, P.: Receptor modeling of ambient particulate matter data
517 using positive matrix factorization: review of existing methods, J. Air Waste Manage.
518 Assoc., 2007.

519 Stein, A.F., Draxler, R.R, Rolph, G.D., Stunder, B.J.B., Cohen, M.D., and Ngan, F.: NOAA's
520 HYSPLIT atmospheric transport and dispersion modeling system, Bull. Amer. Meteor.
521 Soc., 96, 2059-2077, <http://dx.doi.org/10.1175/BAMS-D-14-00110.1>, 2015.

522 Tan, J., Duan, J., Zhen, N., He, K., and Hao, J.: Chemical characteristics and source of size-
523 fractionated atmospheric particle in haze episode in Beijing, Atmos. Res., 167, 24-33,
524 10.1016/j.atmosres.2015.06.015, 2016.

525 Van der A, R. J., Mijling, B., Ding, J., Koukouli, M. E., Liu, F., Li, Q., Mao, H., and Theys,
526 N.: Cleaning up the air: Effectiveness of air quality policy for SO₂ and NO_x emissions in
527 China, Atmos. Chem. Phys. Discuss., doi:10.5194/acp-2016-445, in review, 2016.

528 Wan, D., Han, Z., Yang, J., Yang, G., and Liu, X.: Heavy metal pollution in settled dust
529 associated with different urban functional areas in a heavily air-polluted city in North
530 China, Int. J. Environ. Res. Public Health, 13, E1119, doi: 10.3390/ijerph13111119, 2016.

531 Wang, H.-J. and Chen, H.-P.: Understanding the recent trend of haze pollution in eastern
532 China: roles of climate change, Atmos. Chem. Phys., 16, 4205-4211, doi:10.5194/acp-16-
533 4205-2016, 2016.

534 Wang, G., Zhang, R., Gomez, M. E., Yang, L., Zamora, M. L., Hu, M., and Li, J.: Persistent
535 sulfate formation from London Fog to Chinese haze, Proc. Natl. Acad. Sci., 113, 13630-
536 13635, doi: 10.1073/pnas.1616540113, 2016.

537 Wang, L. T., Wei, Z., Yang, J., Zhang, Y., Zhang, F. F., Su, J., Meng, C. C., and Zhang, Q.:
538 The 2013 severe haze over southern Hebei, China: model evaluation, source apportionment,
539 and policy implications, Atmos. Chem. Phys., 14, 3151-3173, doi:10.5194/acp-14-3151-
540 2014, 2014.

541 Wang, M., Zhu, T., Zhang, J. P., Zhang, Q. H., Lin, W. W., Li, Y., and Wang, Z. F.: Using a
542 mobile laboratory to characterize the distribution and transport of sulfur dioxide in and
543 around Beijing, Atmos. Chem. Phys., 11, 11631-11645, doi:10.5194/acp-11-11631-2011,
544 2011.

545 Wang, M., Zhu, T., Zheng, J., Zhang, R. Y., Zhang, S. Q., Xie, X. X., Han, Y. Q., and Li, Y.:
546 Use of a mobile laboratory to evaluate changes in on-road air pollutants during the Beijing
547 2008 Summer Olympics, *Atmos. Chem. Phys.*, 9, 8247-8263, doi:10.5194/acp-9-8247-
548 2009, 2009.

549 Wang, Y., Yao, L., Wang, L., Liu, Z., Ji, D., Tang, G., Zhang, J., Sun, Y., Hu, B., and Xin, J.:
550 Mechanism for the formation of the January 2013 heavy haze pollution episode over
551 central and eastern China, *Sci. China Earth Sci.*, 57, 14–25, 2014.

552 Wang, Y. Q., Zhang, X. Y., Sun, J. Y., Zhang, X. C., Che, H. Z., and Li, Y.: Spatial and
553 temporal variations of the concentrations of PM₁₀, PM_{2.5} and PM₁ in China, *Atmos. Chem.*
554 *Phys.*, 15, 13585-13598, doi:10.5194/acp-15-13585-2015, 2015.

555 World Health Organization: Air quality guidelines: global update 2005: particulate matter,
556 ozone, nitrogen dioxide, and sulfur dioxide, World Health Organization, 2006.

557 Wu, J., Zhang, P., Yi, H., and Qin, Z.: What causes haze pollution? An empirical study of
558 PM_{2.5} concentrations in Chinese cities, *Sustainability*, 8, 132, doi:10.3390/su8020132,
559 2016.

560 Wu, S., Lu, A., and Li, L.: Spatial and temporal characteristics of minimum temperature in
561 winter in China during 1961–2010 from NCEP/NCAR reanalysis, *Theor. Appl. Climatol.*,
562 108, 207–216, doi: 10.1007/s00704-011-0525-6, 2012.

563 Wu, X., Huang, W., Zhang, Y., Zheng, C., Jiang, X., Gao, X., and Cen, K.: Characteristics
564 and uncertainty of industrial VOCs emissions in China, *Aerosol Air Qual. Res.*, 15, 1045-
565 1058, doi: 10.4209/aaqr.2014.10.0236, 2015.

566 Xie, Y. L., Hopke, P. K., Paatero, P., Barrie, L. A., and Li, S. M.: Identification of Source
567 Nature and Seasonal Variations of Arctic Aerosol by positive matrix factorization, *J.*
568 *Atmos. Sci.*, 56, 249–260, 1999a.

569 Xie, Y. L., Hopke, P. K., Paatero, P., Barrie, L. A., and Li, S. M.: Identification of source
570 nature and seasonal variations of Arctic aerosol by the multilinear engine, *Atmos. Environ.*,
571 33, 2549-2562, doi.org/10.1016/S1352-2310(98)00196-4, 1999b.

572 Yang, K., Dickerson, R. R., Carn, S. A., Ge, C., and Wang, J.: First observations of SO₂ from
573 the satellite Suomi NPP OMPS: Widespread air pollution events over China, *Geophys. Res.*
574 *Lett.*, 40, 4957–4962, 2013.

- 575 Zhang, J. J. and Samet, J. M.: Chinese haze versus Western smog: lessons learned, *J. Thorac.*
576 *Dis.*, 7, 3, doi: 10.3978/j.issn.2072-1439.2014.12.06, 2015.
- 577 Zhang, K., Chai, F., Zheng, Z., Yang, Q., Li, J., Wang, J., and Zhang, Y.: Characteristics of
578 atmospheric particles and heavy metals in winter in Chang-Zhu-Tan city clusters, China, *J.*
579 *Environ. Sci.*, 26, 147-53, 2014.
- 580 Zhang, Y. L. and Cao, F.: Fine particulate matter (PM_{2.5}) in China at a city level, *Sci. Reports*,
581 5, 14884, doi: 10.1038/srep14884, 2015.
- 582 Zhang, R., Jing, J., Tao, J., Hsu, S.-C., Wang, G., Cao, J., Lee, C. S. L., Zhu, L., Chen, Z.,
583 Zhao, Y., and Shen, Z.: Chemical characterization and source apportionment of PM_{2.5} in
584 Beijing: seasonal perspective, *Atmos. Chem. Phys.*, 13, 7053-7074, doi:10.5194/acp-13-
585 7053-2013, 2013.
- 586 Zheng, G. J., Duan, F. K., Su, H., Ma, Y. L., Cheng, Y., Zheng, B., Zhang, Q., Huang, T.,
587 Kimoto, T., Chang, D., Pöschl, U., Cheng, Y. F., and He, K. B.: Exploring the severe
588 winter haze in Beijing: the impact of synoptic weather, regional transport and
589 heterogeneous reactions, *Atmos. Chem. Phys.*, 15, 2969-2983, doi:10.5194/acp-15-2969-
590 2015, 2015.
- 591 Zheng, G., Duan, F., Ma, Y., Zhang, Q., Huang, T., Kimoto, T., and He, K.: Episode-based
592 evolution pattern analysis of haze pollution: method development and results from Beijing,
593 China, *Environ. Sci. Technol.*, 50, 4632-4641, doi: 10.1021/acs.est.5b05593, 2016.

594 **Table 1.** Statistics of PM_{2.5} mass concentrations.

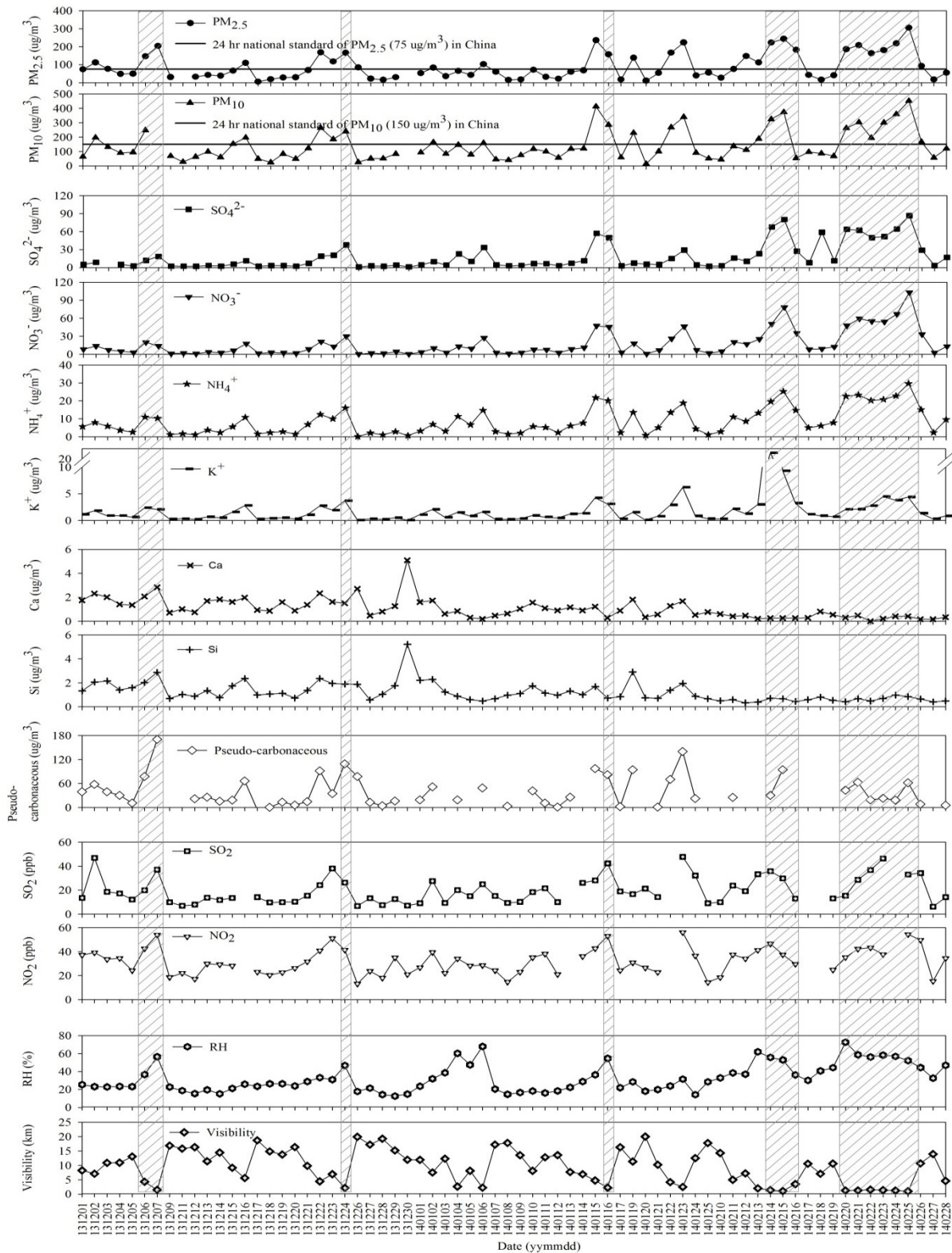
PM _{2.5} mass classification	Number	PM _{2.5} * [$\mu\text{g m}^{-3}$]
Chemical and NMF analysis	70	
Comparison with PM ₁₀ mass	67	89
PM _{2.5} /PM ₁₀ > 0.5	47	113
PM _{2.5} > 75 $\mu\text{g m}^{-3}$ and PM ₁₀ > 150 $\mu\text{g m}^{-3}$	23	168
PM _{2.5} > 75 $\mu\text{g m}^{-3}$ and PM ₁₀ < 150 $\mu\text{g m}^{-3}$	5	113
PM _{2.5} < 75 $\mu\text{g m}^{-3}$ and PM ₁₀ < 150 $\mu\text{g m}^{-3}$	19	39
PM _{2.5} /PM ₁₀ ≤ 0.5	20	31
Haze days [#]	13	198
Red alert	6	218
Orange alert	3	216
No/blue alert	4	168

595 * Average concentration

596 [#] Heavy air pollution alert

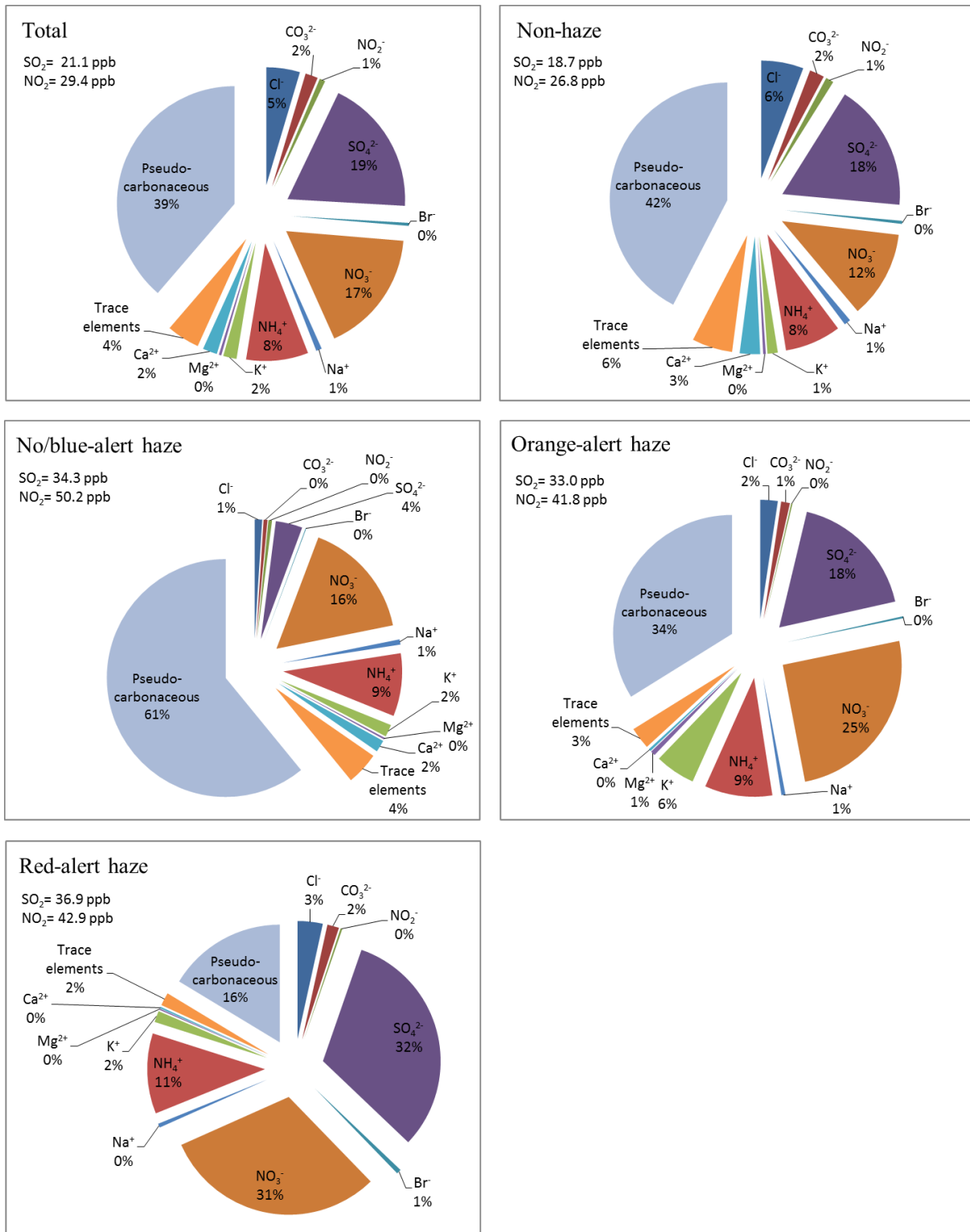
597 **Table 2.** Sources identified by NMF analysis.

Factor	Contribution	Sources
Factor 1	13 %	Soil dust
Factor 2	22 %	Traffic emission
Factor 3	12 %	Biomass combustion
Factor 4	28 %	Industrial emission
Factor 5	25 %	Coal combustion



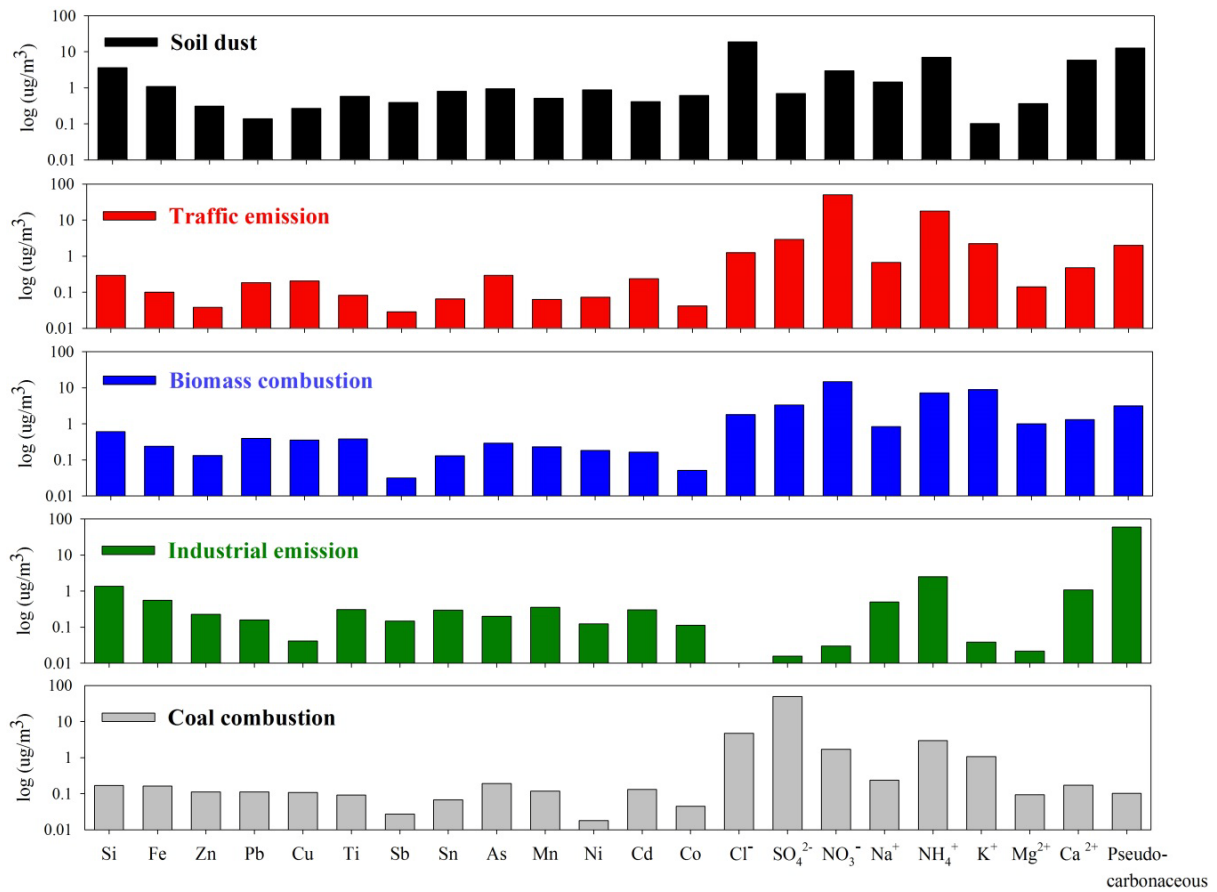
598

599 **Figure 1.** Variations in mass and chemical compositions of PM_{2.5}, PM₁₀ mass, gaseous
 600 precursors, and meteorological parameters measured from Dec. 1, 2013 to Feb. 28, 2014.
 601 Horizontal lines indicate the Chinese national standards of PM concentrations in 24 h and the
 602 vertically shaded regions denote the 13 haze days.



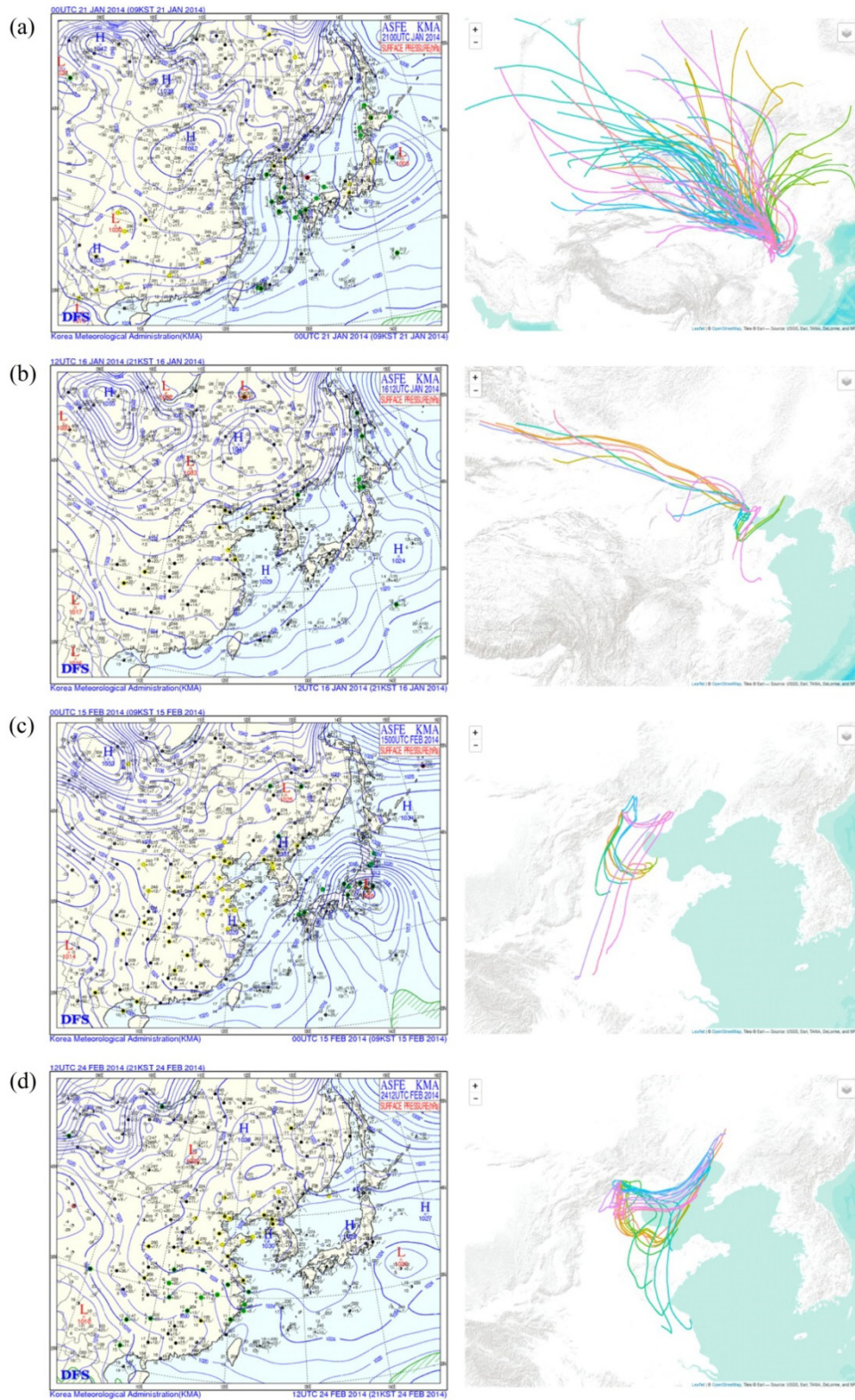
603

604 **Figure 2.** $PM_{2.5}$ mass contributions of water-soluble ions, trace elements, and pseudo-
 605 carbonaceous matter during the entire period (top left), non-haze days (top right), and haze
 606 days at blue-alert (center left), orange-alert (center right), and red-alert (bottom left) warning
 607 levels. The average SO_2 and NO_2 concentrations are also given.



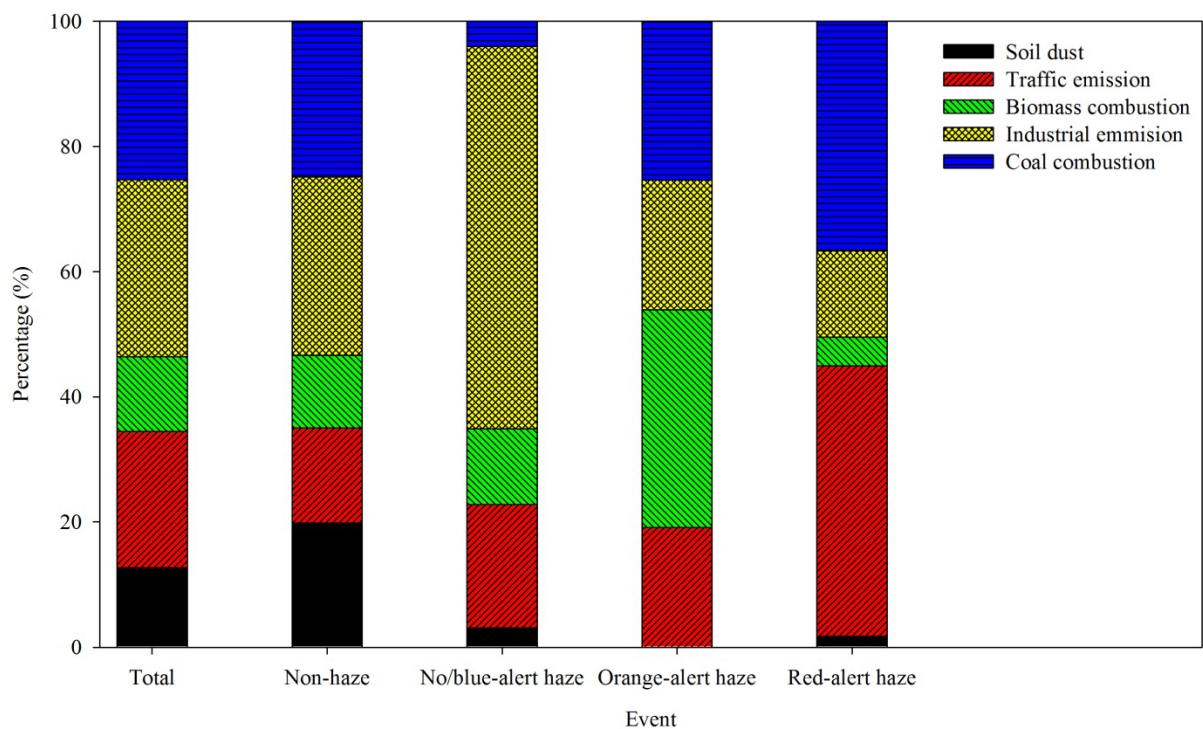
608

609 **Figure 3.** Composition profiles of the five factors identified in NMF analysis.



610

611 **Figure 4.** Surface weather maps and 72-h backward trajectories on days of (a) non-haze (57
 612 days), (b) no/blue-alert haze (4 days), (c) orange-alert haze (3 days), and (d) red-alert haze (6
 613 days). Trajectories were calculated twice a day at 18 and 06 UTC for non-haze days in (a)
 614 and every 6 hours at 12, 18, 24, and 06 UTC for haze days in (b), (c), and (d).



615

616 **Figure 5.** Comparison of source contributions (left to right) over the entire winter, during
 617 non-haze events, and during no/blue-alert, orange-alert, and red-alert haze events.